Surface-wave propagation on isotropic liquids: A study of two-mode structure

C. H. Sohl
Department of Physics and Astronomy, Northwestern University, Evanston, Illinois 60201 and Argonne National Laboratory, Argonne, Illinois 60439

K. Miyano
Argonne National Laboratory, Argonne, Illinois 60439

(Received 6 September 1978)

The dispersion relation for capillary waves on isotropic fluids is written in a dimensionless form appropriate for propagation experiments and solved numerically. Using a recently developed technique to generate and detect capillary waves, the authors have observed a second mode on a highly viscous fluid whose characteristics are in good agreement with theory.

I. INTRODUCTION

It has long been known that surface waves at the liquid-gas interface (capillary waves) provide a convenient probe of the bulk and surface properties of liquids. Experimental techniques to study liquid systems using surface waves fall into two categories: (i) temporal methods (Brillouin scattering) and (ii) spatial methods (propagation experiments). In the former, thermally excited capillary waves interact with incident light causing a momentum and frequency shift of the scattered light. The spectrum of the scattered light at a given momentum transfer is then measured by a variety of means, e.g., a spectrum analyzer and correlator. In the latter, a capillary wave of known frequency is generated, and detected as a function of distance from the generator, thus revealing its propagation characteristics.

The dispersion relation of capillary waves has previously been parametrized into a dimensionless form and numerically solved[1] under the assumption that the momentum of the wave is real, whereas its frequency is complex; a form which is pertinent to the temporal method. In contrast to the dispersion relation of bulk sound waves, the momentum-frequency relation is highly nonlinear. In particular there are two qualitatively distinct modes for a certain range of the parameter.

The predicted mode structure was experimentally observed by Katyl and Ingard[1,2] on various liquids covering the entire range of this parameter. Such a parametrization of the dispersion relation has not to our knowledge been done in a form suitable to the spatial method where frequency is considered real and wave-vector complex. This is understandable since propagation experiments have usually been performed on fluids of low viscosity where an approximated form of the dispersion relation is adequate and a complete solution of the equation is not necessary. We have recently developed a technique to study capillary-wave propagation.[3] The wide dynamic range of our technique has allowed us to observe highly damped waves on viscous fluids conveniently, and hence the necessity arose to solve the equation without approximation.

In this paper we would like to present the result of numerical calculations of the dispersion relation parametrized in the form suitable for propagation experiments. The results show two types of mode for highly viscous fluids, corresponding to the two modes in Brillouin scattering. We will then show data from capillary-wave experiments on a viscous liquid where the two-mode structure is observed for the first time in propagation experiments.

II. THEORY

The derivation of the dispersion relation for surface waves is well known[4,5]; however, it is relevant to our purposes to emphasize certain details. We consider an incompressible isotropic fluid of density ρ, surface tension σ, and shear viscosity η in a Cartesian coordinate system where the z-axis points vertically out of the fluid; the wave-propagation direction is taken to be the x axis located in the fluid surface. If the wave amplitude is small then the linearized Navier-Stokes equation is adequate to describe the fluid motion, subject to boundary conditions at the fluid surface and at $z=-\infty$. We ignore the effects of gravity as they are small at the surface-wave frequencies we usually study. Corrections due to gravity will be discussed later. We assume a plane-wave solution with the fluid displacement in the z direction given by

$$\zeta(x,z,t)=\zeta_0\exp(iqx-St+mz)\,, \tag{1}$$

where

$$q\equiv k+i\alpha \quad \text{and} \quad S\equiv S_r+iS_i\,, \tag{2}$$

and k, α, S_r, and S_i are real.[6] The displacement in the x direction is obtained from the incompressibility assumption $\nabla \cdot \vec{v} = 0$. It is found that two values of m satisfy the equations of motion

$$m_1^2 = q^2 \quad \text{and} \quad m_2^2 = q^2 - S\rho/\eta\,, \tag{3}$$

where the boundary condition at $z = -\infty$ requires that we take the proper signs so that

$$\mathrm{Re}(m_{1,2}) > 0\,. \tag{4}$$

The solution is thus a linear combination of two z-dependent terms as

$$Ae^{m_1 z} + Be^{m_2 z}\,. \tag{5}$$

The boundary conditions at the fluid surface imply that such solutions must satisfy the dispersion relation given by Eq. (6):

$$(m_1^2 + q^2)(i\sigma q^3 - 2i\eta S q m_2) - (m_2^2 + q^2) \times [i\sigma q^3 - 2i\eta S q m_1 + (i\rho S^2/q) m_1] = 0\,. \tag{6}$$

We now consider solutions for Eq. (6) assuming that S is purely imaginary, i.e., a condition appropriate to spatial experiments. Following the conventional notation we write S_i as ω. We assume that k, α, and ω are positive, without loss of generality. Then with the substitutions

$$Q \equiv q/(\omega\rho/\eta)^{1/2} \tag{7}$$

and

$$P \equiv (\omega\eta^3/\rho\sigma^2)^{1/2}; \tag{8}$$

Eq. (6) can be parametrized in the form

$$4Q^4 + (1/P)Q^3 - 4iQ^2 - 1 = 4Q^{3+}\sqrt{(Q^2 - i)}\,, \tag{9}$$

where + denotes the square root whose real part is positive. The dispersion relation for surface waves is now in a dimensionless form. By squaring and after some manipulation, Eq. (9) reduces to

$$Q^7 + (1/8P - 2iP)Q^6 - iQ^5 - 3PQ^4 - \tfrac{1}{4}Q^3 + iPQ^2 + \tfrac{1}{8}P = 0\,, \tag{10}$$

which is in a form convenient for numerical analysis. Equation (10) was numerically solved for Q using the Jenkins-Traub three-stage complex algorithm.[7] For a given parameter P there were seven solutions from which the nonphysical ones were rejected using the following criteria: (a) The solutions have to satisfy the original equation (9), (b) condition (4), and (c) $\mathrm{Im}(Q) > 0$ since $\alpha > 0$.

The relevant range of P was determined as follows. As an example in the low damping limit, we may take water at 100 Hz for which $\omega = 628$ sec^{-1}, $\rho = 1$ g/cm^3, $\sigma = 73$ dyn/cm, $\eta = 0.01$ poise, giving $P = 3.4 \times 10^{-4}$. For an example in the high damping limit, we may consider glycerol at 100 Hz for which $\omega = 628$ cm^{-1}, $\rho = 1.26$ g/cm^3, $\sigma \cong 50$ dyn/cm, $\eta \cong 10$ poise (though this latter quantity is highly temperature dependent), giving $P \cong 14$. We then varied P from 10^{-4} to 10^2 with the results shown in Fig. 1; here the solutions are written in a form $Q = Q_r + iQ_i$, with Q_r and Q_i being plotted separately, representing the real and imaginary parts of Q, respectively. Note that for low P values, only one mode Q_1 exists, while for P values greater than $P \cong 0.105$ there are two modes Q_1 and Q_2. The first mode Q_1 approaches a critically or viscous damped solution in which $Q_i = Q_r$, while the second mode is an overdamped solution in which $Q_i > Q_r$.

In the limit $P \to 0$, the slopes of the solutions for Q_{1r} and Q_{1i} approach $\frac{1}{3}$ and 1, respectively, resulting in the usual low viscosity approximation given by

$$k^3 = \rho\omega^2/\sigma \tag{11}$$

and

$$\alpha = \tfrac{4}{3}\eta\omega/\sigma\,. \tag{12}$$

This approximation, however, is not accurate even at $P = 10^{-4}$, where numerical solution gives slopes of 0.333 and 0.987 for Q_r and Q_i, respectively. The curve for Q_i starts deviating from a straight line at a rather low P value. Conversely if one were to use Eq. (12), or equivalently $Q_i = \frac{4}{3}P$, a 3% error would be introduced for Q_i at $P = 10^{-4}$, where $Q_i = 1.29 \times 10^{-4}$. In the limit $P \to \infty$, $Q_{1r} = Q_{1i} \to 0.74$, $Q_{2r} \to 0.236$, and $Q_{2i} \to 0.428$.

On low-viscosity liquids such as water, it is easy to see why propagation experiments can never detect the second mode; even if waves of frequency 10 kHz could be generated and detected P would still only be 3.4×10^{-3}, well below the appearance of the second mode at $P \cong 0.105$. Because P is

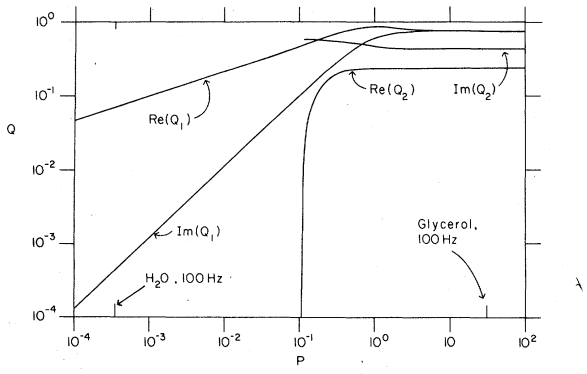

FIG. 1. Solution to the dispersion relation for surface waves in a dimensionless form. Q_r and Q_i are the real and imaginary parts of Q, respectively. Gravitation is neglected.

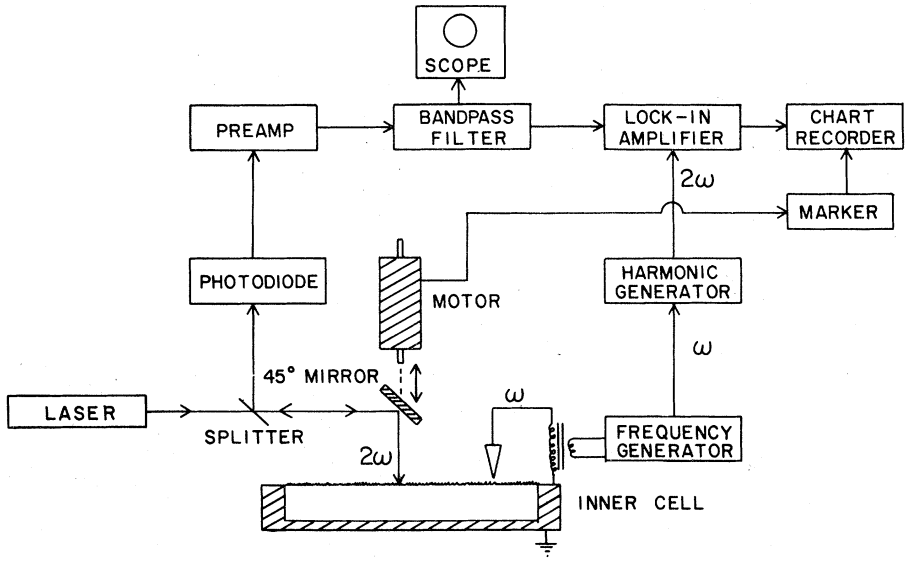

FIG. 2. Block diagram of experimental setup.

proportional to $\eta^{3/2}$ it is expected that changes in fluid viscosity give changes in Q which are more important than those due to frequency changes. As an example we can note that at higher temperatures the viscosity of glycerol is low enough to give values of P in the single-mode region, $P < 0.105$, while at room temperatures glycerol falls well into the two-mode region, $P > 0.105$.

The second mode for large P is not a surface wave in a strict sense because the real part of the wave vector is less than the imaginary part. In fact the form $\exp(iqx + qz)$ implies that the wave propagates *into* the fluid rather than being localized near the surface. A similar situation occurs, for instance, at a solid-fluid interface where a Rayleigh mode on the solid is coupled into the bulk fluid mode[8] (sometimes called a Stonely mode). Thus the energy near the surface is continuously taken away into the bulk. In the literature, the term "leaky mode" is sometimes used for such waves.

Equation (6) defines a hypersurface in a four-dimensional space (k, α, S_r, S_i). The intersection of this surface with a plane $\alpha = 0$ (temporal experiments) and that with a plane $S_r = 0$ (spatial experiments) are qualitatively similar. Thus, there are two modes in the high-viscosity limit in both cases, the upper branch in Fig. 1 of Ref. 1 corresponding to the second mode and the lower branch to the first model, although there are no quantitative relations. In the low-viscosity limit, we have $\alpha \to 0$ and $S_r \to 0$. Therefore, there is no distinction between the two intersections and both reduce to Eq. (11).

As a final point for discussion we show that Fig. 1 can be used to deduce fluid viscosity and surface tension from measurements of wave number k and attenuation coefficient α at a particular wave frequency $\omega/2\pi$. From Fig. 1 it can be seen that the ratio of wave number to attenuation k/α (which is equal to Q_r/Q_i), is a monotonically decreasing function with increasing P. Thus by simply forming k/α we can locate the corresponding value of P uniquely. With a known P value, the ratio R

$$R \equiv (k + i\alpha)/(Q_r + iQ_i) = (\omega\rho/\eta)^{1/2} \tag{13}$$

can also be calculated. Since we then have two equations, Eqs. (8) and (13), for two unknowns, σ and η, we can find unique values for them provided ρ is measured separately. The procedure is simple and there are no approximations.

III. EXPERIMENT

The details of the experimental apparatus will appear elsewhere,[3] but a brief description of the main features is appropriate here. With our apparatus schematically shown in Fig. 2 a sharp metal wedge is carefully positioned very close to the fluid surface (≪1 mm) and an ac voltage is applied to the wedge. Due to electrocapillarity, the fluid (whose dielectric constant is higher than the gas above) tends to rise up to the region of intense electric field at the tip of the wedge. Surface tension and gravitation oppose this motion. Because the strength of the electrocapillarity is proportional to the square of the applied voltage, the surface wave is generated at twice the applied frequency. The deflection of a specularly reflected laser beam from the corrugated surface, which acts like a rocking mirror, was detected by a position sensing photodiode and a phase sensitive detector, as seen in Fig. 2. A mirror mounted on a translation stage was driven by a low rpm dc motor to scan the laser beam and thus sample the wave charac-

teristics as a function of distance from the generator.

Because the generator and detector are essentially noiseless (having no mechanically moving parts) and because the vibration isolation of the apparatus consists of a 2300-kg electromagnet floated from the floor on pneumatic cushions, the noise level is very low. We could detect amplitude changes by factors of 10^3 routinely even when wave amplitudes at the generator were well within the linear regime of the Navier-Stokes equation.

In order to study the two mode structure at high P, we used a viscous vacuum pump fluid, Convaclor-8, (Consolidated Electrodynamics Corp.) for it is chemically stable and the viscosity is insensitive to the temperature. Static measurements indicated a density of 1.4 g/cm^3, a bulk shear viscosity of 3.8 poise, and a surface tension of 42 dyn/cm, giving $P=3.73$ at 100 Hz. Thus at 100 Hz it was expected that a two-mode structure would be observed.

Experiments were carried out at surface wave frequencies of 20, 100, and 400 Hz. Two traces whose phases were 90° apart were taken at each frequency. They were completely reproducible. We then attempted to fit the two traces at each frequency with the functional forms given by

$$Y_1(x)=\sum_{j=1}^{2} A_j e^{-\alpha_j x}\cos(k_j x+\phi_j) \tag{14}$$

and

$$Y_2(x)=\sum_{j=1}^{2} A_j e^{-\alpha_j x}\cos(k_j x+\phi_j-\tfrac{1}{2}\pi), \tag{15}$$

respectively. The parameters A_j, α_j, k_j, and ϕ_j represent the wave amplitude, attenuation, wave number, and phase, respectively. The result of such a fit is seen in Fig. 3 which shows the data taken at 20 and 100 Hz and the calculated values from Eqs. (14) and (15) in circles. A fit was also attempted where only one mode was assumed. This is shown as triangles in Fig. 3. It is clear that a second slowly damped and long-wavelength mode is necessary to avoid zero crossing toward the end of the traces where the signal is well above noise level. We believe that this is the first clear cut indication of the second mode in propagation experiments.

Figure 4 gives the results of the experiments at 20, 100, and 400 Hz, showing the fit values for Q_t and Q_r versus the numerical predictions. The P values were calculated from the known surface

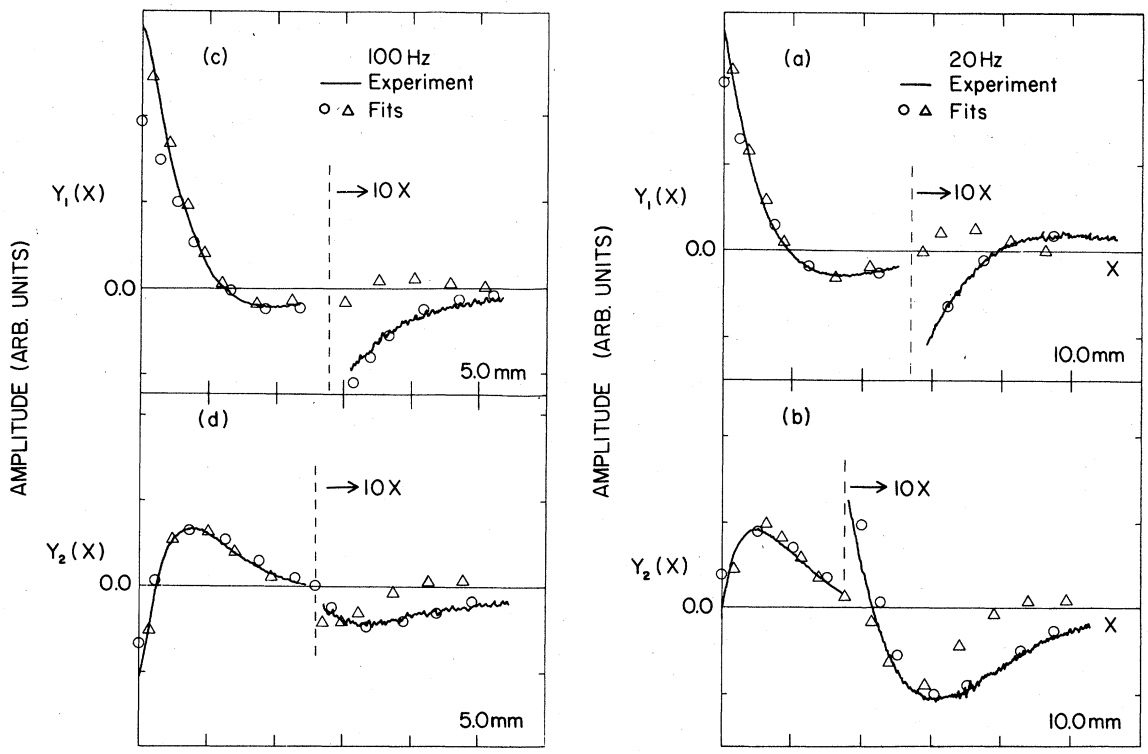

FIG. 3. Experimental data and points representing a single-mode fit (triangles), and a two-mode fit (circles) of the form (14) and (15). (a) and (b) at 20 Hz and (c) and (d) at 100 Hz with $\frac{1}{2}\pi$ phase difference.

wave frequencies and ρ, σ, and η obtained from our static measurements. The solid curve is an enlargement of the high P region of Fig. 1. The dashed curve is a gravitational correction. Since the gravitational force cannot be parametrized in terms of P and Q the correction depends on the specific values of η, σ, ρ, and ω. The gravitational correction is small (~1%) at 100 Hz but it is significant at 20 Hz. The mode structure, however, is not altered by the gravitational effects.

Although the agreement between the experiments and the theory is reasonably good, a systematic discrepancy is clear; measured Q_1 values tend to be larger than predicted while Q_2 values smaller. At the moment we do not known the cause of this phenomenon. This tendency is common for all data analyzed including data taken from glycerol, silicon oils, and other viscous fluids. The effect of the boundary was found to be unimportant because a small trough (4 cm diameter and 0.5 cm deep) gave the same results as a larger trough (7 cm diameter and 8 cm deep).

A similar parametrization is possible for capillary waves on anisotropic fluids involving three shear viscosities. A numerical analysis of the parametrized equation and an experimental study using nematic liquid crystals are in progress.

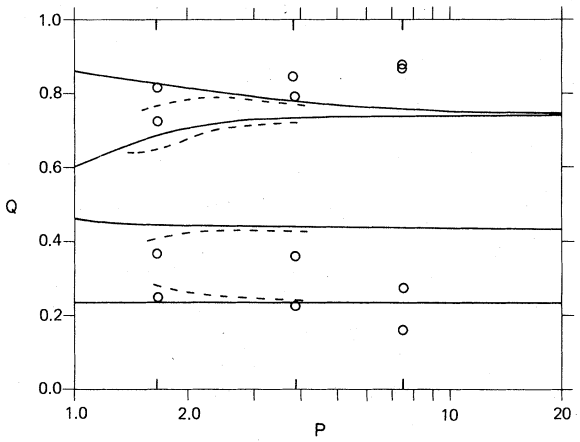

FIG. 4. Comparison between experimental measurements of Q_r, Q_i, and theory based on static measurements. Note that the vertical axis is not logarithmic. The solid curve is an enlargement of Fig. 1. The dashed curve includes a gravitational correction. The open circles are measurements at 20, 100, and 400 Hz from left to right.

ACKNOWLEDGMENTS

We appreciate valuable suggestions by B. M. Abraham, J. B. Ketterson, J. A. Mann, and George K. Wong, and the assistance of D. D. Koelling in computational problems. One of us (CHS) would like to thank the Argonne Center for Educational Affairs for support. This paper was based on work performed under the auspices of the U.S. Department of Energy.

[1]R. H. Katyl and U. Ingard, Phys. Rev. Lett. 19, 64 (1967).

[2]R. H. Katyl and U. Ingard, in *In Honor of Philip K. Morse*, edited by H. Feshback and K. Uno Ingard, (MIT Press, Cambridge, Mass., 1969).

[3]C. H. Sohl, K. Miyano, and J. B. Ketterson, Rev. Sci. Instrum. 49, 1464 (1978).

[4]R. S. Hansen and J. Ahmad, in *Progress in Surface and Membrane Science*, edited by J. F. Danielli, M. D. Rosenberg, and D. A. Cadenhead, (Academic, New York, 1971), Vol. 4.

[5]L. D. Landau, E. M. Lifshitz, in *Fluid Mechanics* (Pergamon, London, 1959), p. 237.

[6]The time factor is written in this particular way for easy comparison with Ref. 1.

[7]M. A. Jenkins and J. F. Traub, Numer. Math. 14, 252 (1970).

[8]See, for instance, H. Uberall, in *Physical Acoustics*, edited by W. P. Mason and R. N. Thurston (Academic, New York, 1973), Vol. X, p. 7.